International Journal of Geotechnical Earthquake Engineering
Volume 14 • Issue 1

Liquefaction Behavior of Typical River Channel Deposit in Kolkata City

Sanjay Prasad, Katihar Engineering College, India
Abhishek Mondal, Baruipur Government Polytechnic, India
Narayan Roy, Jadavpur University, India*
Ramendu Bikas Sahu, Jadavpur University, India

ABSTRACT

Liquefaction susceptibility of river channel deposit in Kolkata city is studied using laboratory cyclic triaxial tests. River channel deposit, which supports a large part of rapidly growing urbanization of Kolkata city, mainly consists of sandy soil with little amount of silt. Cyclic triaxial tests have been performed on this soil sample with varying relative density, confining pressure, and cyclic strain amplitude. Results are presented to show how these parameters influence the pore water pressure generation within soil. Relative density, confining pressure and cyclic strain amplitude are found to affect the pore pressure generation characteristics in the soil, and the number of cycles required to reach liquefaction phenomena vary significantly. Finally, pore pressure generation characteristics are modeled using a hyperbolic model and a pore pressure generation equation is proposed for the typical river channel deposit soil. The model exhibits a certain threshold value of cyclic strain amplitude, up to which the initial rate of pore pressure generation decreases and then increases.

KEYWORDS

Confining Pressure, Cyclic Triaxial Tests, Liquefaction, Pore water pressure, River Channel Deposit, Sands

1. INTRODUCTION

Liquefaction is an exciting topic and active area of research in geotechnical earthquake engineering, although it is quite complex phenomena to be fully understood. The topic initially gained attention following the widespread damage due to liquefaction as a result of Alaska (1964) and Niigata earthquakes (Fukuoka, 1966; Seed, 1968). During liquefaction, soil experiences an increased deformation due to the reduction in effective confining stress when there is a build-up of high excess pore water pressure. Liquefaction generally occurs only in saturated clean sand. Fine grained soils do not generally liquefy (Krammer, 1996). Cohesionless soil deposit sometimes contains significant fine contents and some field observations also exhibit the liquefaction occurrence in sandy-silt/silty-sand type of soils after earthquake event (Ishihara et al., 1980; Boulanger et al., 1999; Orense et al., 2011; Cox et al., 2013). Since then, the study on the liquefaction characteristics of sandy-silt/ silty-sand type of soils has received much attention.

DOI: 10.4018/IJGEE.329249 *Corresponding Author

Several methods of liquefaction potential evaluation are available and these methods mainly utilize different geotechnical data from field tests (Seed and Idriss, 1971; Youd et al., 2001; Idriss and Boulanger, 2006). In-situ shear wave velocity serves an alternative to penetration test in the liquefaction susceptibility evaluation (Andrus and Stokoe, 2000; Youd et al., 2001; Andrus et al., 2004). In order to study the liquefaction susceptibility of soil under controlled conditions in the laboratory, cyclic triaxial apparatus is used worldwide. It can be used to study the influence of different parameters on liquefaction susceptibility (Chien et al., 2000; Arab et al., 2002; Xenaki V.C. and Athanasopoulos G.A, 2003; Ravishankar et al. 2005; Paul et al., 2007; Stamatopoulos, 2010; Kumar et al., 2014; Kumar et al., 2020). Effect of presence of different percentage of silt content in sandy soils has also been studied by several researchers in laboratory using cyclic triaxial (Polito and Martin, 2001; Xenaki and Athanasopoulos, 2003; Stamatopoulos, 2010; Karim and Alam, 2014; Wei and Yang, 2019). Uniform clean sand deposits are quite hard to find as very often this deposit exists with certain percentage of silt content. Now as the behavior of a soil deposit under cyclic loading may significantly vary for different types of soil deposit depending on the nature, so, each of them needs to be characterized for cyclic loading in the laboratory under controlled condition.

In this study, an effort has been given to study the liquefaction characteristics of typical RCD in Kolkata city. The Kolkata city is extended up to an area of ~ 185 sq.km and the population as per the Census of India, 2011 is about 4.5 million. More than 80% of the city area is covered and congested with buildings, business areas, hospitals, and schools. Most of the constructions of the city is without any proper planning and quite old (Nandy 2007). With the expansion of urban habitation, it is now extremely important to study the liquefaction characteristics of a soil prior to any construction over it. The alluvial Gangetic deposit mainly forms the subsoil of Kolkata city. In the city, two different types of subsurface stratifications are observed: normal Kolkata deposit (NKD) and RCD. In NKD, a thick layer of silty clay/ clayey silt up to a depth of ~14m and after that a deposit of stiff/very stiff/ hard/very hard clay to a depth of 40-50m with intermediate sand layers is observed. On the other hand, along the course of Adiganga channel The RCD is observed. In this stratification, medium to dense sandy deposit is obtained up to a significant depth (Roy and Sahu, 2012).

Few studies have been carried out on the liquefaction behavior of Gangetic sand. Nilay and Chakrabortty (2018) studied the liquefaction behavior of Ganga River sand with the influence of non-plastic silt. The study concludes that with 10% silt content the rate of excess pore water pressure generation decreased initially, after that increased significantly with 30% silt content and then reduced for 100% silt content. Das and Chakrabortty (2021) conducted strain controlled cyclic triaxial tests on cohesionless soil collected from middle Ganga plain to study the influence of effective confining stress, shear strain amplitude and frequency of motion. The study concludes that the cyclic shear strain amplitude significantly affects the dynamic properties and liquefaction strength, whereas, effective confining stress and frequency of motion have minor influence at large strain. Naik et al. (2021) studied the efficacy of biochar in liquefaction mitigation of Ganga sand. The results pointed out the 30 to 50% increase in loading cycles for soils treated with biochar in comparison with clean Ganga sand. Das and Chakrabortty (2022) presented a study to model the large strain cyclic behavior of cohesionless soil from MGP using regression, statistical and neural network methods. The authors find neural network to be more precise in predicting cyclic behavior of soil. Sharika and Kumari (2023) also studied the liquefaction behavior of Ganga sand. The study reveals that the state of soil and effective confining stress are the major contributing factor in the liquefaction susceptibility.

The liquefaction potential at different locations of Kolkata city is studied by Chakraborty et al. (2004) using Artificial Neural Network (ANN) for different PGA levels, concludes that the RCDs are the most vulnerable to liquefaction. Now the need of a controlled laboratory study to analyze the cyclic behavior of Kolkata-RCD is essential in order to understand the soil behavior in case of an occurrence of actual future earthquake event. Soil sample which typically represents the RCD is collected from Industrial Training Institute (ITI) compound, Tollygunge, Kolkata. Now, the liquefaction characteristics of this typical RCD has been studied using controlled laboratory cyclic triaxial tests. An effort has

also been made to study the influence of different parameters, such as confining pressure, relative density, and cyclic shear strain amplitude, on liquefaction phenomena. Generation of excess pore water pressure during an earthquake loading bears the most crucial information about the initiation of liquefaction phenomena. Finally, the work has been extended to model the pore water pressure generation characteristics using a hyperbolic model proposed by Kondner (1963).

2. TESTING MATERIAL AND PROCEDURE

2.1 Grain Size Distribution (GSD)

The test sample which typically represents the RCD of Adi Ganga Channel is collected from the ITI compound, Tollygunge. The sample is taken out from 1.5 to 4m depth below ground surface by making boreholes of diameter 150mm using a hand driven auger. Disturbed sand samples were collected from the threads of the auger after it was lifted by using hand operated winch. The physical properties (specific gravity, mean grain size, uniformity coefficient (C_u) etc.) of the soil sample are determined after the collection of the soil sample from the site. Figure 1 depicts the typical grain size distribution curve of the collected soil and Table 1 shows the estimated values of different physical properties. The silt content in this soil is obtained as 17.82% (less than 75μm) from the GSD curve and the mean particle size $D_{50} = 0.12$ mm. The GSD curve has been superimposed with boundaries for partial liquefiable zone (PHRI, 1997) and boundaries for highly liquefiable zone (PHRI, 1997). It can be found that GSD curve of RCD falls between highly liquefiable boundaries of PHRI.

Pycnometer test is performed to determine the specific gravity and it is found to be 2.39. Relative Density and Modified Proctor Tests are performed to obtain the maximum dry density and the values are: $\gamma_{dmax} = 1.525$ and 1.715 gm/cc, respectively. For the calculation purpose, higher value of γ_{dmax} (1.715 gm/cc) is adopted. The γ_{dmin} value obtained from relative density test is 1.157 gm/cc.

Now to study the effect of different relative densities on liquefaction phenomena, target relative densities of 25%, 50% and 75% are planned to prepare using 'Moist Tamping Method'. The details on sample preparation have been discussed in details in the following section. Now the value of a relative density, $R_d = 25\%$, signifies the loosest state of the sand, and a value of $R_d = 75\%$ means the densest state of the sand sample.

2.2 Sample Preparation

Moist tamping (MT) method is adopted for the preparation of sample at desired relative densities. An oven-dried batch of sand has been mixed thoroughly with de-aired water to achieve certain percentage of moisture content. This small amount of water has been added (5% to 10% by weight) to the dry sand sample to make the sample denser as water acts as lubricating agent between sand particles. If more than 10% of water is added, it would be difficult to construct a sample in the mould. If dry sand is compacted then the friction between the sand particles would not allow the sand sample for much more densification, so it would be difficult to achieve the targeted relative density. The moist sand has been compacted in 3 layers to achieve the required relative density forming a specimen with 75 mm diameter and 150 mm height. Each batch was dumped onto two membrane-lined pedestals encapsulated inside a spilt mould. Compaction has been performed by a tamper on each layer until the prescribed height would be reached. Porous stone with filter paper at bottom and top of split mould was given before placing it to cyclic triaxial testing machine. Table 2 provides the details about how the relative densities of 25%, 50% and 75% have been achieved.

2.3 Testing Program

Testing program has been decided to study the three influencing parameters, relative density, effective confining pressure, and cyclic shear strain amplitude, in strain control cyclic triaxial test. Thus, the total combinations of test come out to be 27. Three different relative densities are selected for

Figure 1. Grain size distribution curve of the soil sample

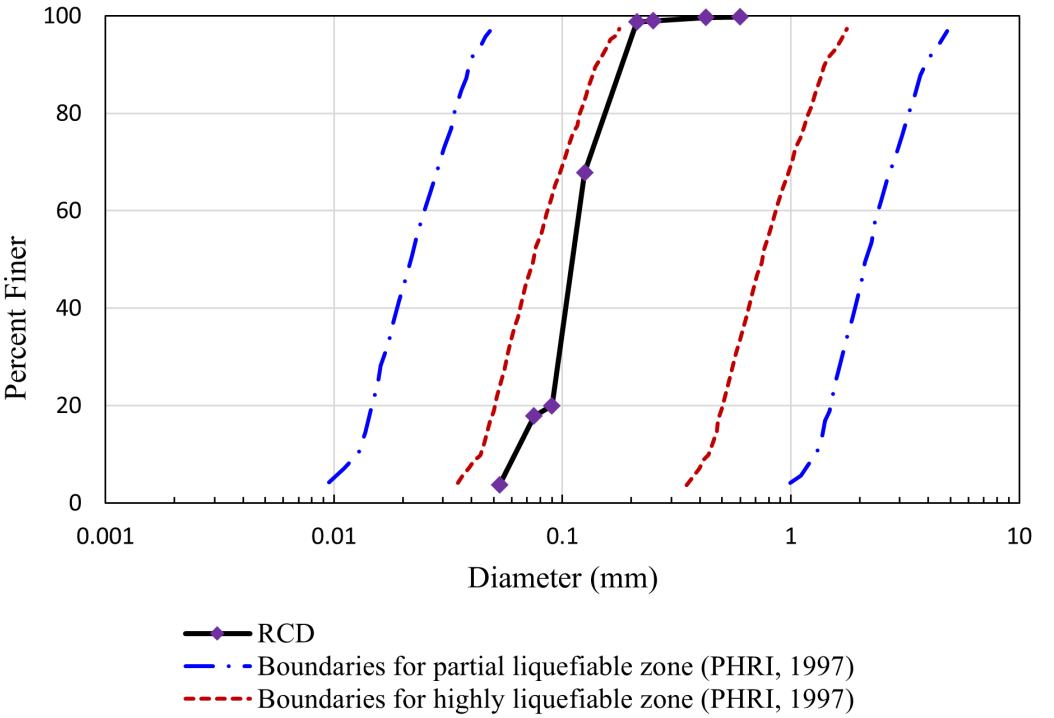

Table 1. Physical properties of the soil sample

Physical properties	Estimated Values
Specific gravity of soil solid, G_s	2.39
Mean grain size, D_{50}	0.12 mm
Coefficient of uniformity (C_u) Coefficient of curvature (C_c)	2.15 1.099
Maximum, γ_{dmax} Minimum dry density γ_{dmin}	1.715 gm/cc 1.157 gm/cc
Relative density, R_d	25%, 50% and 75%
USCS Classification	SP-SM

the study, i.e., 25%, 50% and 75%. These densities are achieved by moist tamping method already discussed in the previous section. Now, each relative density sample has been tested for three different effective confining pressures (σ_{3c}'), viz, 50, 100, 150 kPa. Again, to study the effect of cyclic shear strain amplitude, a sample with a particular relative density and confining pressure has been tested with three different cyclic shear strains amplitude, i.e., 0.5%, 0.67% and 0.83% (or displacements ±0.75mm, ±1.00mm and ±1.25mm respectively). So, a total of 27 numbers (3×3×3 = 27) of tests have been conducted in the laboratory. The detailed test program has been presented in Table 3.

Table 2. Sample preparation by moist tamping method

Parameters	Values		
No. of Layer	3	3	3
No. of tamping for each layer	10	30	55
Target dry Density (gm/cc)	1.259	1.382	1.530
Weight of sample achieved (gm)	886.64	970.64	1052.64
Volume of sample (cc)	662.7	662.7	662.7
Actual unit weight obtained (gm/cc)	1.338	1.464	1.588
Actual dry density obtained (gm/cc)	1.274	1.396	1.515
Target Moisture Content (%)	5	5	5
Actual Moisture Content achieved (%)	4.98	4.86	4.82
Target Relative density (%)	25	50	75
Actual Relative Density achieved (%)	28.426	52.607	72.617

2.4 Testing Procedure

A Cyclic Triaxial Test System (HS-28.610) supplied by HEICO with a combination of hydraulic and pneumatic technology has been used for the testing. The instrument uses a hydraulic system to apply major principal stress during a dynamic test, on the other hand pneumatic system is utilized while to apply minor principal stress. The complete instrument setup has been presented in Fig. 2. The size of the sample for all the tests has been adopted as 75 x 150mm. Before transferring a sample to triaxial cell, a sample is prepared with outmost care with a specific relative density using moist tamping method. After that, the triaxial chamber is filled with water till water overflows an open valve at the top. Once the water is filled in the chamber, the sample is saturated under a confining stress of 280 kPa and with a back pressure of 250 kPa for about two and half hours for R_d =75%, for two hours for R_d = 50% and for one and half hours for R_d = 25%. After the saturation of sand sample is over, consolidation comes in the next phase. Consolidation of the sand sample is performed under a cell pressure of 350 kPa and with a back pressure of 250 kPa for about half an hour. Once the consolidation phase gets completed, the test is performed at a desired effective confining pressure (σ'_{3c}) by adjusting cell and back pressure. If the desired effective confining pressure is 100 kPa, then the cell pressure is adjusted to 350 kPa and back pressure is adjusted to 250 kPa. Proper attention has been given so that back pressure doesn't fall below 250 kPa during or after saturation. It is so because the sand sample has been saturated with a back pressure of 250 kPa, and if the back pressure is reduced below 250 kPa then the water from the sand sample will come out and the sample will become partially saturated.

Now after the consolidation phase gets over, the sample is then subjected to cyclic loading. The excitation frequency has been selected as 1Hz. Sometimes the loading frequency is chosen based on the soil types. Excitation frequency of 1 Hz is commonly used to study the liquefaction characteristics of sandy soil in the laboratory. Now if the soil samples contain considerable amount of silt or the soil is fine grained, greater time is required for pressure equalization, in that case lowest possible loading frequency is selected as excitation frequency (Bray and Sancio, 2006; Hyde et al., 2006; Jakka et al., 2010). Finally, the specified cyclic loading is applied to the specimen till the liquefaction occurs.

Table 3. Details of test programme in this study

No. of Tests	Relative Density (%)	Cell Pressure (kPa)	Back Pressure (kPa)	Effective Confining Pressure (kPa)	Cyclic Shear Strain (%)
1	**75**	350	300	50	0.50
2					0.67
3					0.83
4		400		100	0.50
5					0.67
6					0.83
7		450		150	0.50
8					0.67
9					0.83
10	**50**	350	300	50	0.50
11					0.67
12					0.83
13		400		100	0.50
14					0.67
15					0.83
16		450		150	0.50
17					0.67
18					0.83
19	**25**	350	300	50	0.50
20					0.67
21					0.83
22		400		100	0.50
23					0.67
24					0.83
25		450		150	0.50
26					0.67
27					0.83

3. RESULTS AND DISCUSSION

Figures 3 to 5 present the laboratory test results of a typical RCD for different relative density, confining pressure, and cyclic strain amplitude, respectively. For 25% relative density, cyclic deviatoric stress vs no. of cycles, stress vs strain and excess pore water pressure vs no. of cycles are presented in Figs. 3(a1), (a2) and (a3). Figs. 3(b1), (b2) and (b3) and Figs. 3(c1), (c2) and (c3) presents the same for 50% and 75%, respectively. The results clearly depict the development of excess pore water pressure which ultimately leads to the liquefaction (i.e., effective confining pressure becomes equal with the generated excess pore pressure). For specimen with 25% relative density, i.e., sample prepared in loosest state, the generation of excess pore pressure is rapid. Sample prepared in densest state, i.e., $R_d = 75\%$, requires higher number of cycles to reach to the state of initial liquefaction. For example,

Figure 2. The laboratory cyclic triaxial test setup

at cyclic shear strain of 0.5% and at effective confining pressure of 50 kPa, a failure cycle of ~25 is observed for loose sand (R_d = 25%) and a failure cycle of ~80 is observed for dense sand (R_d = 75%). One quite significant observation is that for loose soil sample, the development of pore water pressure is quite rapid and nearly same rate of generation of pore water pressure is observed and continues till it reaches the initial liquefaction. On the other hand, for dense soil sample, two stages of pore water pressure generation are observed (Figs. 3b3 & c3). The first stage is quite rapid like loose soil specimen and in second stage, the rate of generation of pore water pressure gets reduced. This is possibly due to the dilative behavior of dense sand which results in a different rate of pore pressure generation in the second stage.

Figure 4 show the results for varying confining pressure (σ_{3c}'), i.e., 50, 100 and 150 kPa while the other two parameters are constant (R_d = 25%, Amplitude: 0.75mm). At a particular soil relative density (R_d) and confining pressure (σ_{3c}'), with the increase in confining pressure, more numbers of cycles are required to initiate the liquefaction (Figs. 4a3, b3 & c3). In case of pore pressure generation, for first two effective confining pressures, i.e., σ_{3c}'= 50 kPa and 100 kPa, nearly same rates of development of pore water pressure are observed (Figs. 4a3 & b3). But for effective confining pressure of 150 kPa, two different stages of pore water pressure generation are observed similarly like the pore water pressure generation of dense soil specimen. So, at higher effective confining stress, even the loose soil may exhibit the rate of pore pressure generation pattern similar to dense soil. Figure 5 show the results for varying cyclic strain amplitude, i.e., 75, 100 and 125mm while rest two parameters are constant (σ_{3c}':50 kPa, R_d = 50%). With the increase in cyclic shear strain amplitude, lesser numbers of cycles are required for the initiation of liquefaction phenomena (Figs. 5a3, b3 & c3).

3.1 Failure in Terms of Number of Cycles

3.1.1 Effect of Relative Density

Now to get a clear insight on how each parameter affects the liquefaction phenomena, effect of relative density, confining pressure and cyclic shear strain amplitude are presented separately. To study the effect of relative density in the liquefaction resistance of RCD of Kolkata, cyclic triaxial tests have been performed by preparing the soil samples at three different relative density values. Again, each

Figure 3. Results obtained from cyclic triaxial tests for (a) R_d = 25% (σ_{3c}':100 kPa, Amplitude: 0.75 mm), (b) R_d = 50% (σ_{3c}':100 kPa, Amplitude: 0.75 mm) and (c) R_d = 75% (σ_{3c}':100 kPa, Amplitude: 0.75 mm)

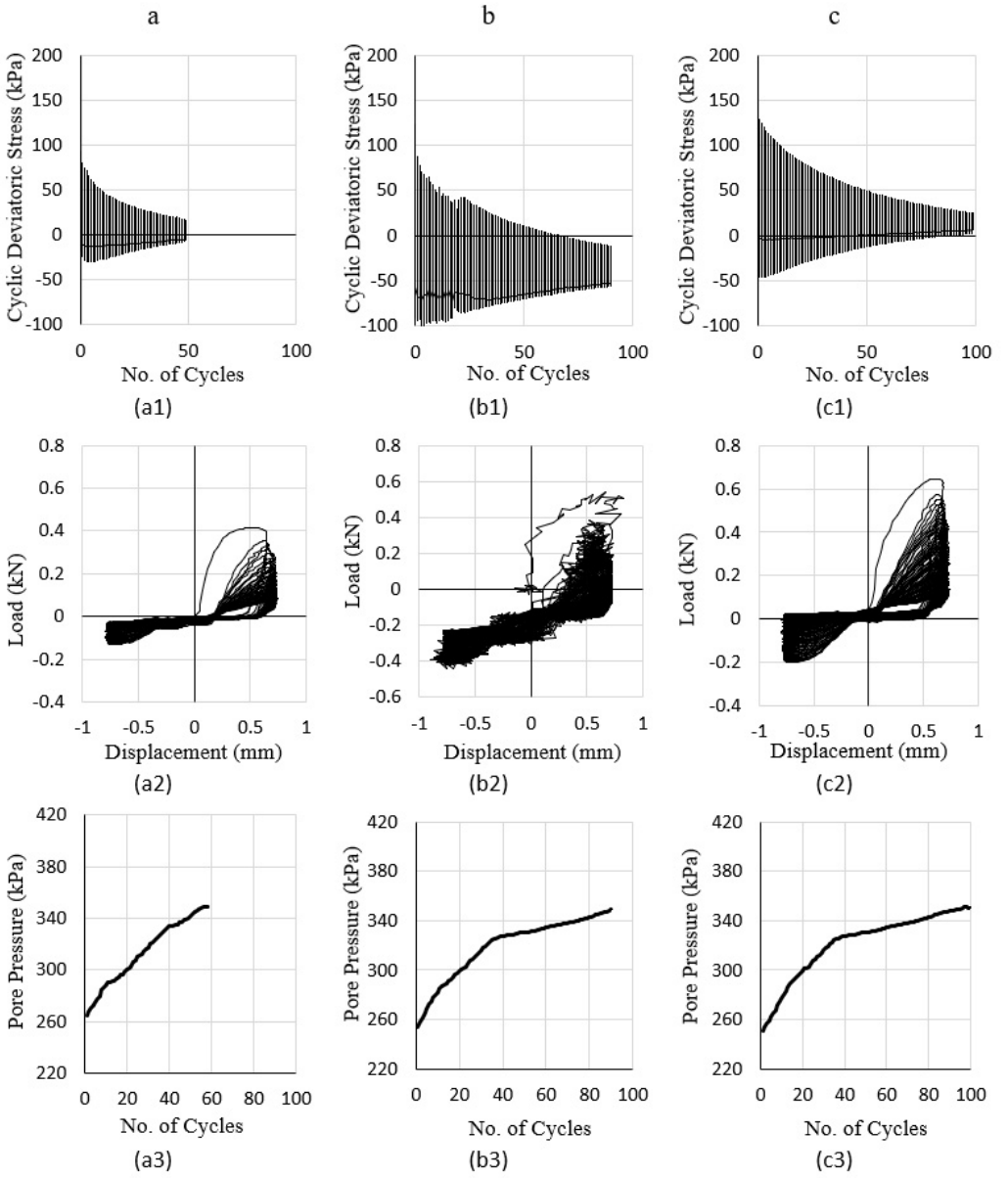

relative density sample has been tested by varying the cyclic shear strain and effective confining pressure at three different values. Figure 6 presents the number of failure cycles obtained from the tests for different relative densities, effective confining pressures (σ_{3c}'= 25, 50 and 75) and shear strain amplitudes (0.5%, 0.67% and 0.83%). The plot clearly reveals that a smaller number of cycles are required to initiate the liquefaction in the case of 25% relative density but this number of cycles increases as the relative density increases to 75%. This is somehow intuitive, as the relative density of a particular soil sample increases, it leads to the increase in the soil shear strength and the number

Figure 4. Results obtained from cyclic triaxial tests for (a) σ_{3c}':50 kPa (R_d = 25%, Amplitude: 0.75 mm), (b) σ_{3c}':100 kPa (R_d = 25%, Amplitude: 0.75 mm) and (c) σ_{3c}':150 kPa (R_d = 25%, Amplitude: 0.75 mm)

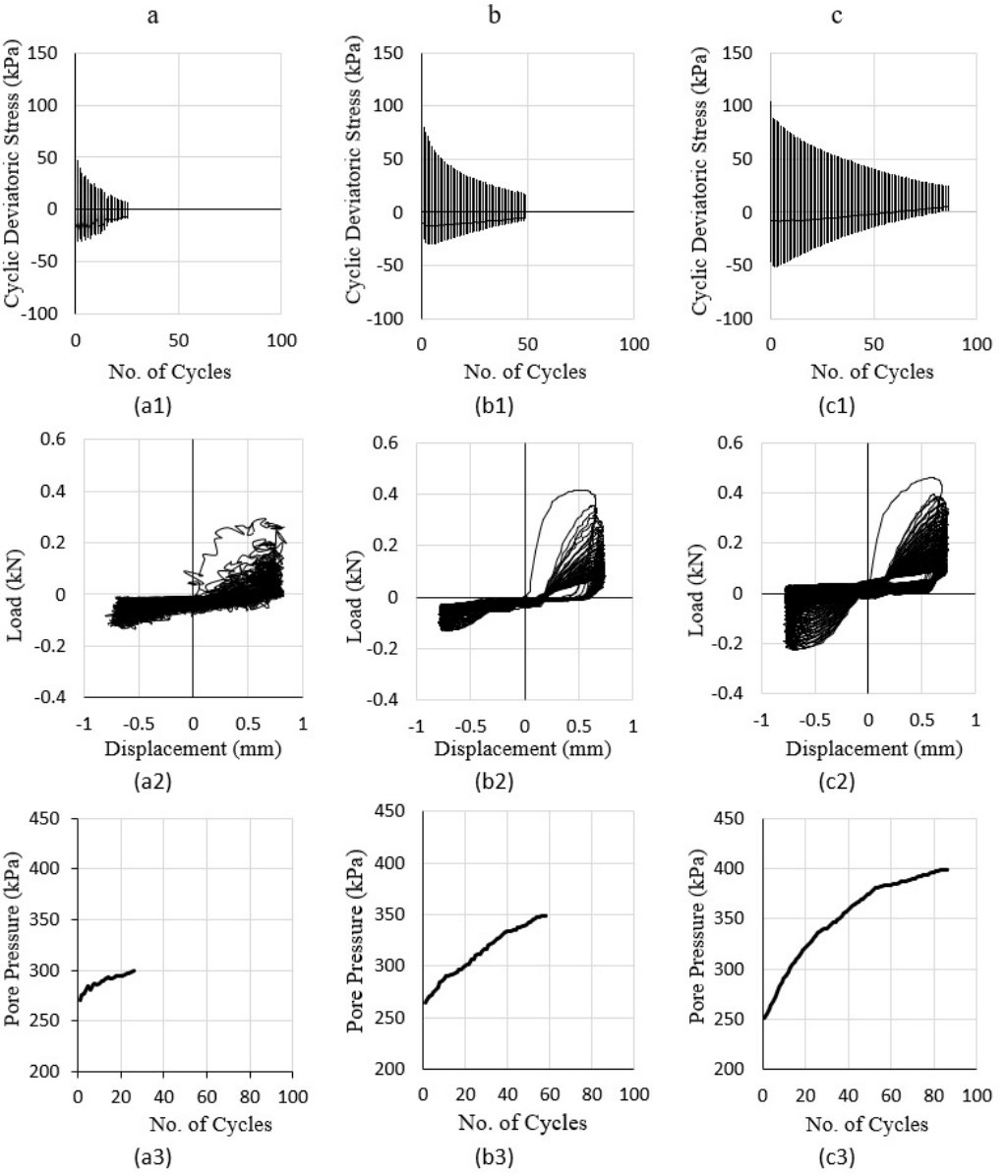

of cycles at failure also increases to initiate the liquefaction. It clearly signifies that possibility of liquefaction gets reduced with the increase in relative density of soil.

3.1.2 Effect of Confining Pressure

Another plot has been prepared (Fig. 7) in terms of number of cycles at failure and effective confining pressure for different considered relative densities and shear strain amplitudes. It can be observed that at low effective confining pressure, σ_{3c}'= 50 kPa, lesser number of cycles are required for liquefaction, and number of cycles increase with the increase in effective confining pressure. So,

Figure 5. Results obtained from cyclic triaxial tests for: (a) Amplitude: 0.75 mm (σ_{3c}':50 kPa, R_d = 50%), (b) Amplitude: 1.00 mm (σ_{3c}':50 kPa, R_d = 50%) and (c) Amplitude: 1.25 mm (σ_{3c}':50 kPa, R_d = 50%)

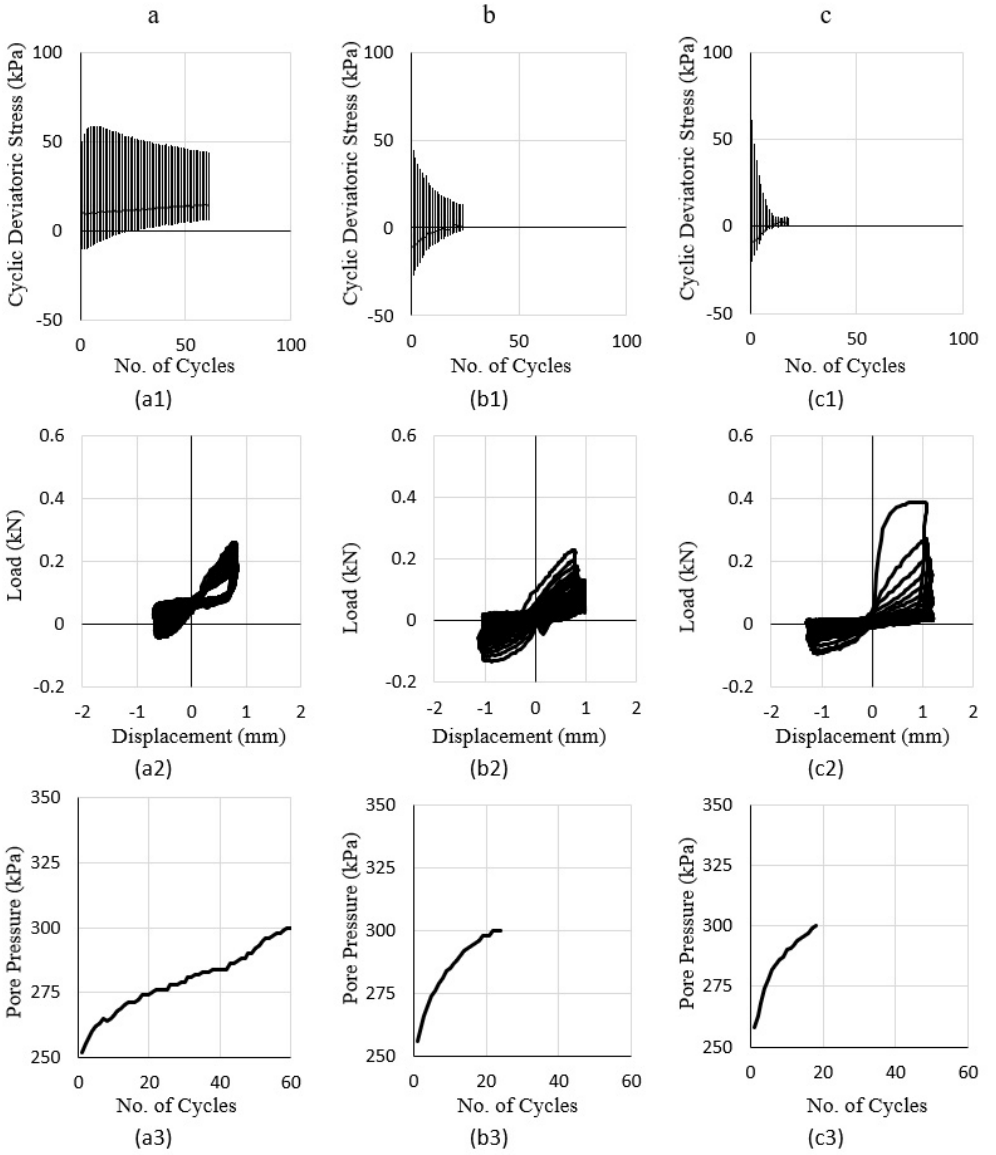

the liquefaction resistance of the sand increases with the increase in confining pressure. This is so because the higher confining pressure led to higher shear strength of soil. Results also portray that the number of failure cycles for all the three considered effective confining pressures and relative densities is quite very high for low cyclic shear strain amplitude (0.5%). The maximum variation (62 cycles) in number of failure cycles is observed for the lowest relative density, i.e., for $R_d = 25\%$. So, it can be stated that the RCD of Kolkata city may exhibits large variation in the initial liquefaction; and the effective confining pressure may play a major role in liquefaction behavior in its loosest state with low cyclic strain amplitude.

Figure 6. Cyclic behavior of typical RCD of Kolkata city with different relative densities

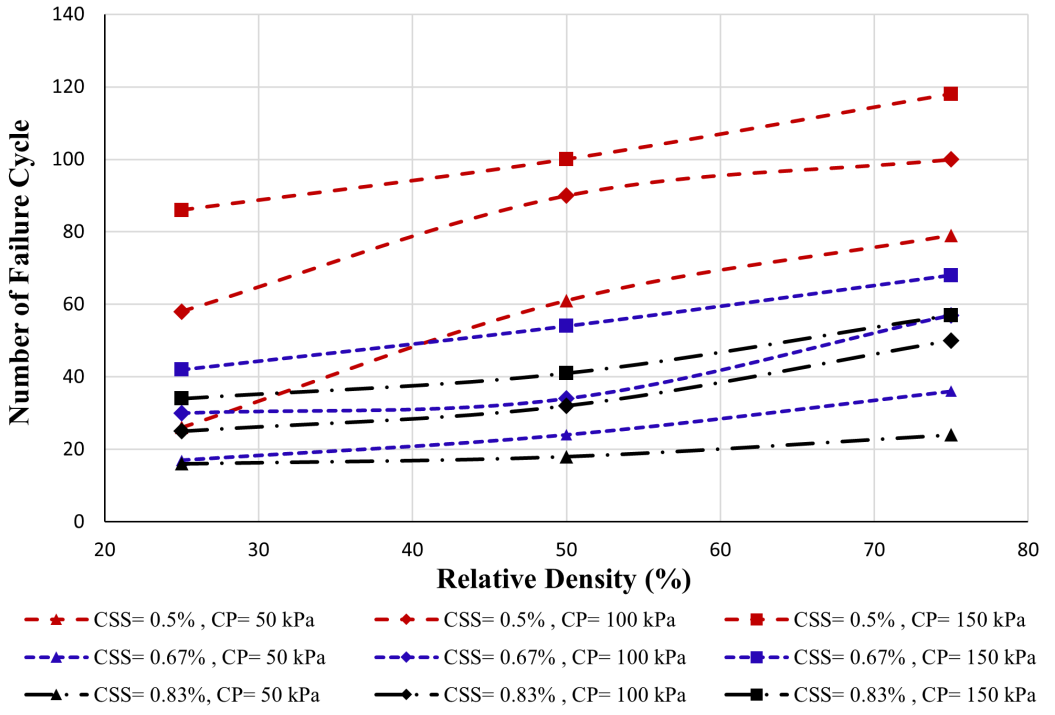

Figure 7. Cyclic behavior of typical RCD of Kolkata city with different confining pressures

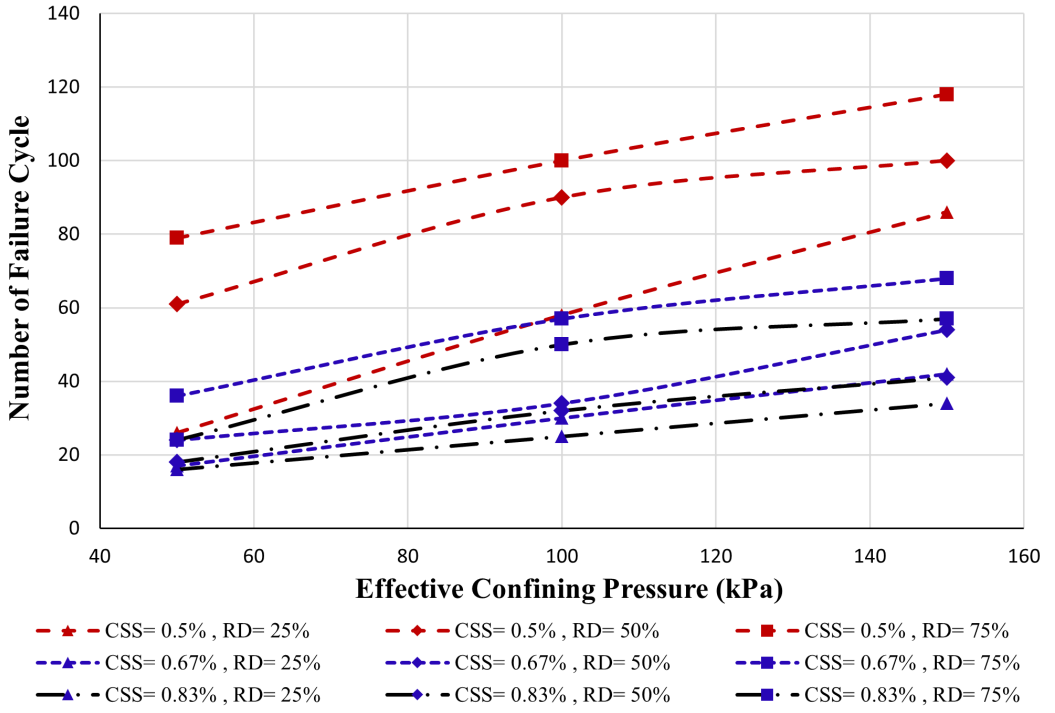

3.1.3 Effect of Cyclic Shear Strain (CSS)

Figure 8 presents the plot of test results which reflect the effect of cyclic shear strain amplitude in terms of number of failure cycles for three different relative densities and effective confining pressures. It can be observed that when the value of cyclic shear strain is low, higher number of cycles are required for liquefaction, whereas, at higher shear strain amplitude, liquefaction starts at lower number of cycles. It signifies that with the increase in cyclic shear strain amplitude, the strength of soil reduces quite rapidly and it leads to liquefaction even at lesser number of cycles. Another interesting observation can be made from this plot. At lower cyclic shear strain amplitude (i.e., 0.5%) and at lower effective confining pressure (50 kPa), the variation in the number of failure cycles from loosest state to densest state is quite very large. So, another conclusion based on this can be made that if the RCDs of Kolkata city experience any cyclic loading at low confining stress and cyclic shear strain amplitude, the soil may exhibit large variation in the failure cycles from its loosest state to densest state. So, in this case the liquefaction resistance of soil can be increased significantly by simply increasing the relative density of the soil deposit. On the contrary, at higher cyclic shear strain amplitudes with low effective confining pressure, the relative density does not play a major role in the liquefaction resistance of RCD. In this scenario simply increasing the relative density of soil may not be a fruitful option to increase the liquefaction resistance.

3.2 Pore Pressure Generation Characteristics

Once the variation of pore pressure generation of RCD is quantified from different combinations of tests, an effort has also been made to model the pore pressure generation characteristics using a hyperbolic model proposed by Kondner (1963). If stress is plotted along Y-axis and strain is plotted along X-axis, it will result in a hyperbolic relationship. Based on standard triaxial test, the model approximates the stress-strain behavior by the following hyperbolic relation (Eq. 1):

Figure 8. Cyclic behavior of typical RCD of Kolkata city with different shear strain amplitudes

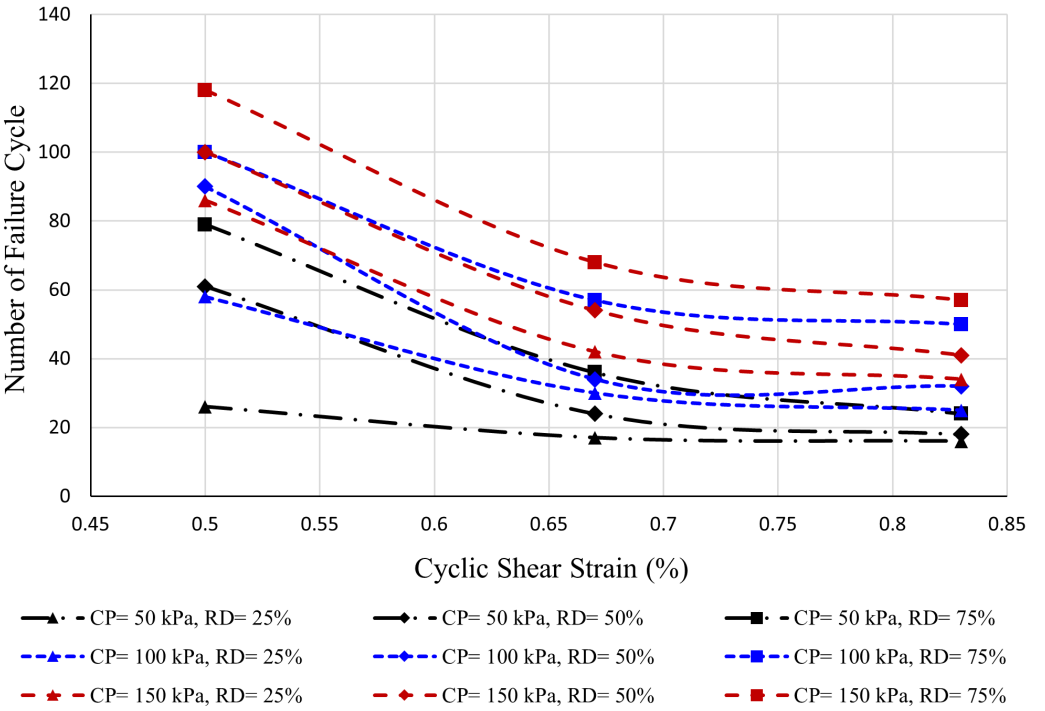

$$\sigma_d = \sigma_1 - \sigma_3 = \frac{\varepsilon_1}{a + b\varepsilon_1} \quad (1)$$

where, σ_1, σ_3 are the major and minor principal stresses and ε_1 is the major principal strain.

If (ε_1/σ_d) is plotted along Y-axis and ε_1 along X-axis, then it will lead to a straight line from which two parameters 'a' and 'b' can easily be calculated. Here, 'a' is the inverse of the initial tangent modulus and 'b' is the inverse of the asymptotic value of the hyperbolic curve and is related to soil strength.

In order to develop a pore pressure generation model, the variation of ($\Delta u/\sigma_c$') with respect to (N/N_f) is plotted and the curve shows an asymptotic nature. The graph for amplitude 1.25 mm and R_d= 50% has been shown in Fig. 9 for reference. The nature of the graph shows that it is clearly asymptotic in nature and the basic equation (Eq. 2) for this graph will be as follows:

$$(\Delta u/\sigma'_c) = \frac{N/N_f}{a + b\left(N/N_f\right)} \quad (2)$$

Where, Δu= Change in pore pressure

σ_c'= Effective confining pressure
N= N^{th} number of cycles
N_f= Number of cycles to failure

The aim here is to find the unknown parameters 'a' and 'b'. Hence, a plot is prepared [(N/N_f)/ ($\Delta u/\sigma_c$)] along Y-axis and (N/N_f) along X-axis to get a straight-line plot and hence to find the

Figure 9. Variation of normalized pore water pressure cycles (N/N_f) to the pore water pressure ratio ($\Delta u/\sigma_c$) for amplitude = 1.25 mm and R_d= 50%

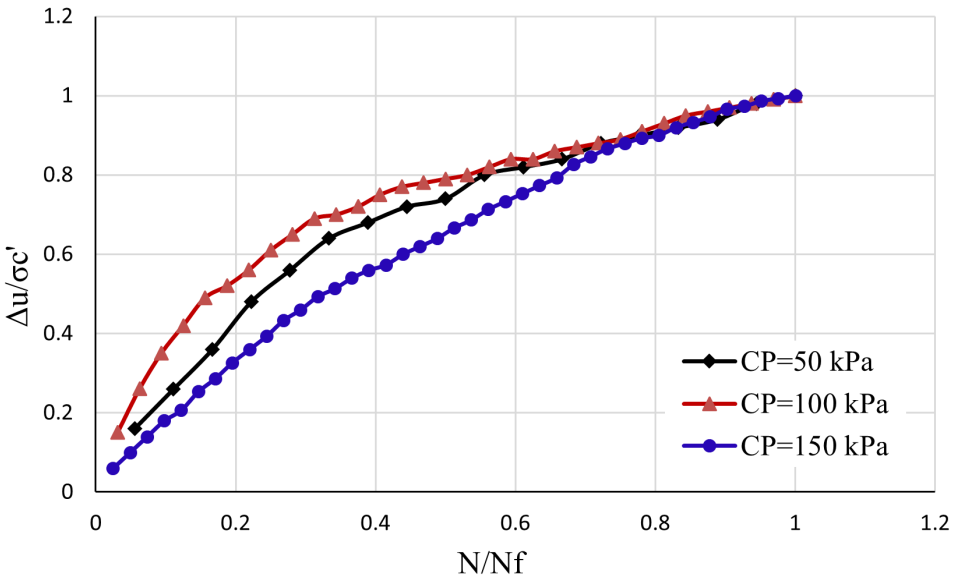

parameters 'a' and 'b'. Figures 10(a)-(c) present the straight line fit for cyclic strain amplitude 0.75, 1.0 and 1.25mm. From these 3 plots, the parameters 'a' and 'b' of the hyperbolic model can easily be found out and the values are listed in Table 4.

From Table 4, it can be observed that, the parameters are more or less independent of relative density but depend upon the cyclic axial strain amplitude. With the increase of cyclic strain, the 'a' value increases first and then decreases and on the contrary, 'b' value decreases first and then increase. Hence, it can be said that with the increase in the strain amplitude, the initial rate of pore pressure generation decreases up to a certain threshold value of cyclic strain and then increases. On the other hand, the magnitude of maximum generated pore pressure increases up to that certain threshold value of strain and then decreases. As in the present case, it can be concluded that the threshold value lies somewhere in between 1.00 and 1.25 mm i.e., in between cyclic axial strain values of 0.67% and 0.83%.

The pore pressure generation equation (Eq. 3) after the elapse of N number of cycles in hyperbolic model comes out as:

$$\frac{\Delta u}{\sigma_c'} = \frac{N/N_f}{0.55 + 0.42\, N/N_f} \tag{3}$$

Where, Δu = Change in pore pressure

σ_c' = Effective confining pressure

N_f = Number of cycles to failure

4. CONCLUSION

The liquefaction characteristics of typical RCD of Kolkata city is studied through extensive laboratory study using cyclic triaxial tests. The effect of relative density, confining pressure and cyclic shear strain amplitude on liquefaction resistance are studied. And finally, the characteristic of pore water pressure generation is modeled using a hyperbolic model proposed by Kondner (1963). Findings from the entire study are summarized as follows:

i. Relative density seems to play an important role in the liquefaction resistance phenomena of Kolkata RCD. A quite fast increase in pore water pressure is observed till liquefaction for sample with low relative density (R_d = 25%). On the other hand, sample with high relative density (R_d = 50 and 100%) exhibits two different stage of pore pressure generation, in first stage, the rate is quite rapid, but after a certain cycle of loading, the rate slows down in the second stage till it reaches the initial liquefaction.
ii. As the confining pressure increases, liquefaction resistance of the soil sample increases irrespective of the relative density and cyclic shear strain. the variation in the number of failure cycles for all the three considered effective confining pressures and relative densities is quite very high for low cyclic shear strain amplitude (0.5%). The maximum variation (62 cycles) is observed for the lowest relative density, 3i.e., for R_d = 25%. So, it can be stated that the RCD of Kolkata city may exhibit large variation in the initial liquefaction; and the effective confining pressure may play a major role in liquefaction behavior in its loosest state with low cyclic strain amplitude.
iii. Liquefaction resistance of the soil significantly gets affected by the amplitude of cyclic shear strain. At lower cyclic shear strain, liquefaction occurs at higher number of cycles and for high

Figure 10. Hyperbolic Model for (a) Amplitude = 0.75 mm, (b) Amplitude = 1.00 mm and (c) Amplitude = 1.25 mm

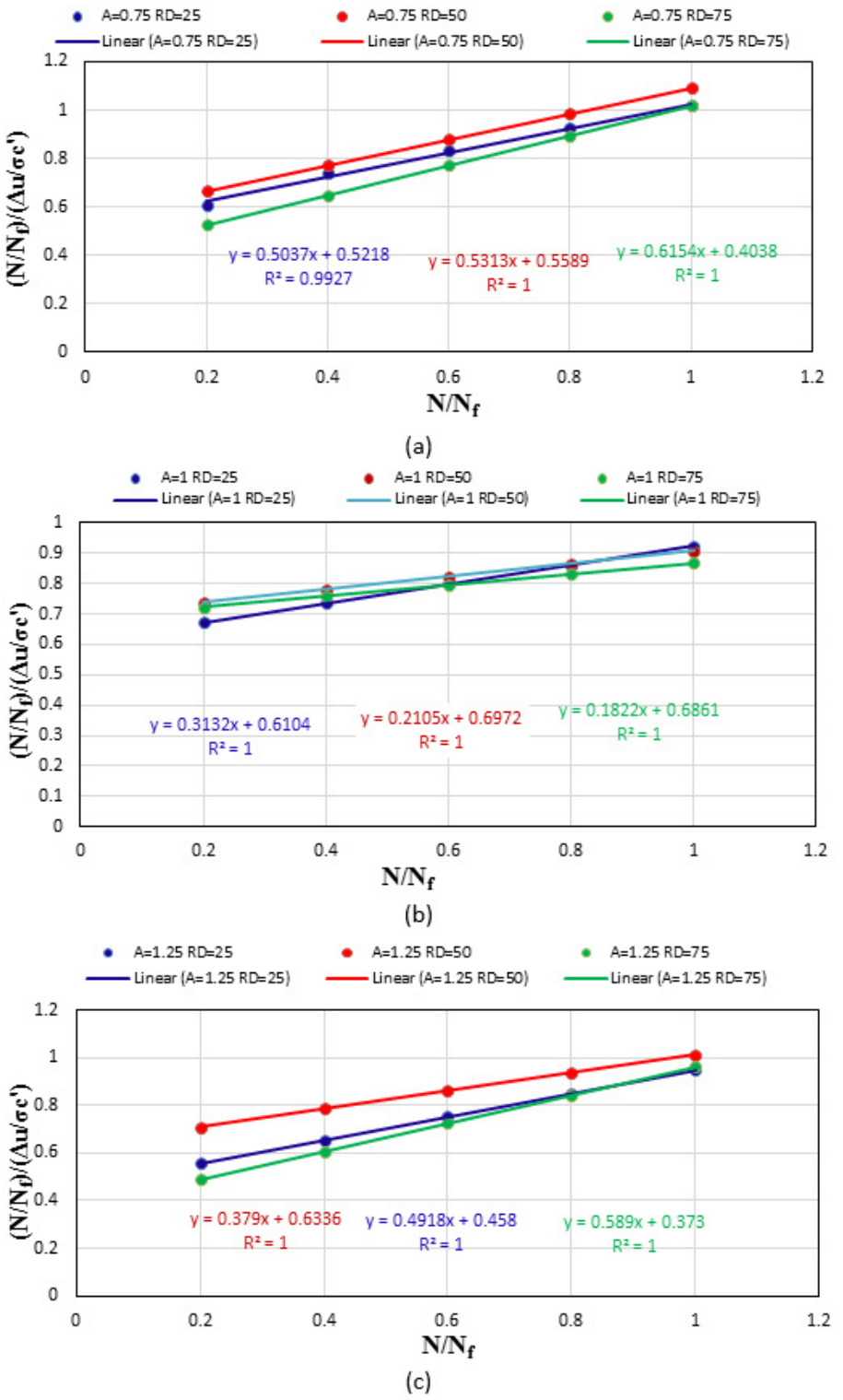

Table 4. Parameters of hyperbolic model

Amplitude (mm) (Strain amplitude)	Relative Density (%)	a-value	b-value	Average of a	Average of b
0.75 (0.5%)	25	0.5218	0.5037	0.4948	0.5501
	50	0.5589	0.5313		
	75	0.4038	0.6154		
1.00 (0.67%)	25	0.6104	0.3132	0.6645	0.2353
	50	0.6972	0.2105		
	75	0.6861	0.1822		
1.25 (0.83%)	25	0.4580	0.4918	0.4882	0.4886
	50	0.6336	0.3790		
	75	0.3730	0.5890		
			Average values	0.5492	0.4240

cyclic shear strain, liquefaction occurs at lower number of cycles irrespective of relative density and confining pressure. At lower cyclic shear strain amplitude (i.e., 0.5%) and at lower effective confining pressure (50 kPa), the variation in the number of failure cycles from loosest state to densest state is significant. So, it can be stated that if the RCDs of Kolkata city experience any cyclic loading at low confining and cyclic shear strain amplitude, the soil may exhibit large variation in the failure cycles from its loosest state to densest state and by simply increasing the relative density of the soil deposit liquefaction resistance can be increased dramatically. On the contrary, at higher cyclic shear strain amplitudes with low effective confining pressure, the relative density does not play a major role in the liquefaction resistance and simply increasing the relative density of soil may not be a fruitful option to increase the liquefaction resistance.

iv. Pore water pressure generation characteristics are modeled using a hyperbolic model and it is found that 'a' and 'b' parameters are more or less independent of relative density but depend upon the cyclic strain amplitude. With the increase of cyclic strain amplitude, the 'a' value increases first and then decreases and on the contrary, 'b' value decreases first and then increase, and it hints the existence of a certain threshold value of cyclic strain amplitude, up to which the increase in shear strain, the initial rate of pore pressure generation decreases and then increases. On the other hand, the magnitude of maximum generated pore pressure increases up to that certain threshold value of strain amplitude and then decreases. As in the present case, it can be concluded that the threshold value lies somewhere in between 1.00 and 1.25 mm i.e., in between cyclic strain values of 0.67% and 0.83%.

REFERENCES

Andrus, D. A., Piratheepan, P., Ellis, B. S., Zhang, J., & Juang, C. H. (2004). Comparing liquefaction evaluation methods using penetrationVs relationships. *Soil Dynamics and Earthquake Engineering*, *24*(910), 713–721. doi:10.1016/j.soildyn.2004.06.001

Andrus, R. D., & Stokoe, K. H. I. I. II. (2000). Liquefaction resistance of soils from shear-wave velocity. *Journal of Geotechnical and Geoenvironmental Engineering*, *126*(11), 1015–1025. doi:10.1061/(ASCE)1090-0241(2000)126:11(1015)

Arab, A., & Belkhatir, M. (2002). Fines Content and Cyclic Preloading Effect on Liquefaction Potential of Silty Sand: A Laboratory Study. *Acta Polytechnica Hungarica*, *9*(4).

Boulanger, R. W., Mejia, L. H., Myers, M. W., & Idriss, I. M. (1999). Behavior of a fine-grained soil during the Loma Prieta earthquake [reply]. *Canadian Geotechnical Journal*, *36*(3), 584. doi:10.1139/t99-025

Census of India. (2011). Provisional population totals (Paper 1). Office of Registrar General & Census Commissioner, India.

Chakraborty, P., Pandey, A. D., Mukerjee, S., & Bharghava, A. (2004). Liquefaction Assessment for Microzonation of Kolkata City. *13th World Conference on Earthquake Engineering, Vancouver, B.C.*, Canada.

Chien, L. K., Oh, Y. N., & Chang, C. H. (2000). Evaluation of Liquefaction Resistance & Liquefaction induced settlement for Reclaimed soil. *13th World Conference on Earthquake Engineering*, (Paper No. 0386). Indian Institute of Technology Kanpur.

Cox, B. R., Boulanger, R. W., Tokimatsu, K., Wood, C. M., Abe, A., Ashford, S., Donahue, J., Ishihara, K., Kayen, R., Katsumata, K., Kishida, T., Kokusho, T., Mason, H. B., Moss, R., Stewart, J. P., Tohyama, K., & Zekkos, D. (2013). Liquefaction at strong motion stations and in Urayasu City during the 542 2011 Tohoku-Oki earthquake. *Earthquake Spectra*, *29*(1_suppl, S1), S55–S80. doi:10.1193/1.4000110

Das, A., & Chakrabortty, P. (2021). Large strain dynamic characteristics of quaternary alluvium sand with emphasis on empirical pore water pressure generation model. *European Journal of Environmental and Civil Engineering*, *26*(12), 5729–5752. doi:10.1080/19648189.2021.1916605

Das, A., & Chakrabortty, P. (2022). Simple models for predicting cyclic behaviour of sand in quaternary alluvium. *Arabian Journal of Geosciences*, *15*(5), 385. doi:10.1007/s12517-022-09639-6

Fukuoka, M. (1966). Damage to civil engineering structures. *Soil and Foundation*, *6*(2), 45–52. doi:10.3208/sandf1960.6.2_45

Hyde, A. F. L., Higuchi, T., & Yasuhara, K. (2006). Liquefaction, cyclic mobility, and failure of silt. *Journal of Geotechnical and Geoenvironmental Engineering*, *132*(6), 716–735. doi:10.1061/(ASCE)1090-0241(2006)132:6(716)

Idriss, I. M., & Boulanger, R. W. (2006). Semi -empirical procedures for evaluating liquefaction potential during earthquakes. *Soil Dynamics and Earthquake Engineering*, *26*(2-4), 115–130. doi:10.1016/j.soildyn.2004.11.023

Ishihara, K., Troncoso, J., Kawase, Y., & Takahashi, Y. (1980). Cyclic strength characteristics of tailings materials. *Soil and Foundation*, *20*(4), 127–142. doi:10.3208/sandf1972.20.4_127

Jakka, R. S., Dutta, M., & Ramana, G. V. (2010). Liquefaction behavior of loose and compacted pond ash. *Soil Dynamics and Earthquake Engineering*, *30*(7), 580–590. doi:10.1016/j.soildyn.2010.01.015

Karim, M. E., & Alam, M. J. (2014). Effect of non-plastic silt content on the liquefaction behavior of sand–silt mixture. *Soil Dynamics and Earthquake Engineering*, *65*, 142–150. doi:10.1016/j.soildyn.2014.06.010

Kondner, R. L. (1963). Hyperbolic Stress–Strain Response: Cohesive Soils. *Journal of the Soil Mechanics and Foundations Division*, *89*(1), 115–143. doi:10.1061/JSFEAQ.0000479

Kramer, S. L. (1996). *Geotechnical earthquake engineering*. Prentice Hall.

Kumar, S. S., Dey, A., & Krishna, M. A. (2020). Liquefaction Potential Assessment of Brahmaputra Sand Based on Regular and Irregular Excitations Using Stress-Controlled Cyclic Triaxial Test. *KSCE Journal of Civil Engineering*, *24*(4), 1070–1082. doi:10.1007/s12205-020-0216-x

Kumar, S.S., Krishna, M.A., & Dey, A. (2014). Dynamic Soil Properties of Brahmaputra sand using Cyclic Triaxial Test. *NES Geocongress on Advances in Geotechnical Engineering*. NES.

Naik, S. P., Choudhury, B., & Garg, A. (2021). Laboratory Investigations of Liquefaction Mitigation of Ganga Sand Using Stable Carbon Material: A Case Study. *International Journal of Geosynthetics and Ground Engineering*, *2021*(7), 89. doi:10.1007/s40891-021-00333-3

Nandy, D. R. (2007). *Need for seismic microzonation of Kolkata megacity.* Workshop on microzonation, Indian Institute of science, Bangalore, India.

Nilay, N., & Chakrabortty, P. (2018). *Evolution in liquefaction strength of ganga river sand due to intrusion of non-plastic silt*. IGC-2018, IISC Bangalore.

Orense, R. P., Kiyota, T., Yamada, S., Cubrinovski, M., Hosono, Y., Okamura, M., & Yasuda, S. (2011). Comparison of liquefaction features observed during the 2010 and 2011 Canterbury earthquakes. *Seismological Research Letters*, *82*(6), 905–918. doi:10.1785/gssrl.82.6.905

Paul, S., & Dey, A. K. (2007). Cyclic Triaxial Testing on Fully & Partially Saturated Soil at Silchar. *4th International Conference on Earthquake Geotechnical Engineering*. USACE.

Polito, C. P., & Martin, J. R. II. (2001). Effects of nonplastic fines on the liquefaction resistance of sands. *Journal of Geotechnical and Geoenvironmental Engineering*, *127*(5), 408–415. doi:10.1061/(ASCE)1090-0241(2001)127:5(408)

PHRI Port & Harbour Research Institute. (1997). *Handbook on liquefaction remediation of reclaimed land, Balkema*. PHRI Port & Harbour Research Institute.

Ravishankar, B. V., & Sitharam, T. G. (2005). *Dynamic Properties of Ahmedabad Sand at Large Strains*. *Indian Geotechnical Congress*, Ahmedabad.

Roy, N., & Sahu, R. B. (2012). Site specific ground motion simulation and seismic response analysis for microzonation of Kolkata. *Geomechanics and Engineering*, *4*(1), 1–18. doi:10.12989/gae.2012.4.1.001

Seed, H. B. (1968). Landslides during earthquakes due to soil liquefaction. *J Soil Mech Found Eng Div*, *94*, 193–260.

Seed, H. B., & Idriss, I. M. (1971). Simplified procedure for evaluating soil liquefaction potential. *Journal of the Soil Mechanics and Foundations Division*, *97*(9, SM9), 1249–1273. doi:10.1061/JSFEAQ.0001662

Sharika, S., & Kumari, S. D. A. (2023). *An Experimental Study on Static and Cyclic Undrained Behaviour of Gangetic Sand*. Indian Geotech J., doi:10.1007/s40098-023-00727-2

Stamatopoulos, C. A. (2010). An experimental study of the liquefaction strength of silty sands interms of the state parameter. *Soil Dynamics and Earthquake Engineering*, *30*(8), 662–678. doi:10.1016/j.soildyn.2010.02.008

Wei, X., & Yang, J. (2019). Characterizing the effects of fines on the liquefaction resistance of silty sands. *Soil and Foundation*, *59*(6), 1800–1812. doi:10.1016/j.sandf.2019.08.010

Xenaki, V.C., & Athanasopoulos, G.A. (2002). *Liquefaction resistance of sand-silt mixtures: an experimental investigation of effect of fines*. NASA.

Xenaki, V. C., & Athanasopoulos, G. A. (2003). Liquefaction resistance of sand–silt mixtures: An experimental investigation of the effect of fines. *Soil Dynamics and Earthquake Engineering*, *23*(3), 183–194. doi:10.1016/S0267-7261(02)00210-5

Youd, T. L., Idriss, I. M., Andrus, R. D., Arango, I., Castro, G., Christian, J. T., Dobry, R., Finn, W. D. L., Harder, L. F. Jr, Hynes, M. E., Ishihara, K., Koester, J. P., Liao, S. S. C., Marcuson, W. F. III, Martin, G. R., Mitchell, J. K., Moriwaki, Y., Power, M. S., Robertson, P. K., & Stokoe, K. H. II. (2001). Liquefaction resistance of soils; summary report from the 1996 NCEER and 1998 NCEER/NSF workshops on evaluation of liquefaction resistance of soils. *Journal of Geotechnical and Geoenvironmental Engineering*, *127*(10), 817–833. doi:10.1061/(ASCE)1090-0241(2001)127:10(817)